Can Baseline Parapapillary Atrophy Morphology Predict Future Glaucoma Progression?—An OCT Glaucoma Imaging Study

MIN GU HUH, YOON JEONG, YOUNG IN SHIN, KI HO PARK, AND JIN WOOK JEOUNG

• PURPOSE: To investigate glaucoma progression based on Optical Coherence Tomography (OCT) Guided Progression Analysis (GPA) according to baseline β-zone parapapillary atrophy (PPA) morphology in glaucoma patients.

• DESIGN: Retrospective cohort study.

• METHODS: Patients over 20 years of age who had been diagnosed with primary open-angle glaucoma (POAG) at Seoul National University Hospital, Seoul, Korea between 2010 and 2020. This study included POAG patients with a minimum of 5 years of follow-up. We quantitatively measured the baseline β-zone PPA parameters, classified β-zone PPA morphology according to new classification standard we created and analyzed the corresponding GPA progression of the retinal nerve fiber layer (RNFL).

• RESULTS: A total of 210 patients with POAG (mean age: 53.8 years) were enrolled in the study. The mean follow-up period was 9.8 years. The average value of the baseline mean deviation in visual field perimetry was -2.48 dB. Longer radial extent and larger angular extent of β-zone PPA were significantly associated with progression on GPA, as was the presence of disk hemorrhage. Among the 4 classified β-zone PPA morphologies (Crescent type 1 & 2, Solar-eclipse type 1 & 2), the Solar-eclipse type 2 group showed the highest progression. A Kaplan-Meier survival analysis demonstrated significant differences among the 4 types.

• CONCLUSIONS: The larger the radial and angular extents of β-zone PPA, the more progression that was shown on OCT GPA. Furthermore, significant differences in progression were noted based on the morphological type of β-zone PPA. Our findings indicate that baseline β-zone PPA parameters and morphology are valuable predictors of future glaucoma progression. (Am J Ophthalmol 2024;267: 19–29. © 2024 Elsevier Inc. All rights are reserved, including those for text and data mining, AI training, and similar technologies.)

Meeting Presentation: None.
Accepted for publication May 30, 2024.

From the Department of Ophthalmology, Seoul National University Hospital (M.G.H., Y.J., Y.I.S., K.H.P., J.W.J.), Seoul, South Korea; Department of Ophthalmology, Seoul National University College of Medicine (M.G.H., Y.J., Y.I.S., K.H.P., J.W.J.), Seoul, South Korea; Department of Ophthalmology, Yeungnam University Hospital (M.G.H.), Daegu, South Korea; Department of Ophthalmology, Gachon University Gil Medical Center (Y.I.S.), Incheon, South Korea

Inquiries to Jin Wook Jeoung, Department of Ophthalmology, Seoul National University Hospital, Seoul National University College of Medicine, 101 Daehak-ro, Jongno-gu, Seoul, 03080, South Korea; e-mail: jeoung@snu.ac.kr

INTRODUCTION

Glaucoma, characterized by optic nerve damage and visual field loss, is a progressive and chronic eye disease that often leads to irreversible blindness if left untreated. Understanding the factors that influence glaucoma progression is crucial for early identification and management of patients at risk. The progression of glaucoma is known to be associated with numerous factors, among which β-zone parapapillary atrophy (PPA) has been extensively implicated in various studies.[1-4]

PPA, manifesting very close to the optic nerve head (ONH), is known to be more extensive in glaucoma patients.[5-9] β-zone PPA is characterized by marked atrophy of the retinal pigment epithelium and choriocapillaris, with good visibility of the sclera and choroidal vessels.[1,2] Examining the impact of β-zone PPA parameters such as angular extent, radial extent, and PPA area on glaucoma, Park et al. discovered a significant association with the increase of visual field defects.[10] Teng et al. reported that in glaucoma patients experiencing both β-zone PPA and VF progression, the location of the largest β-zone PPA was spatially correlated with the area of fastest VF progression in the future.[11]

Furthermore, an increasing body of recent research indicates a connection between β-zone PPA and the subsequent progression of glaucoma. Bak et al., through a long-term observational study, reported that an enlargement of the β-zone PPA area was associated with the progression of glaucoma. Additionally, an increase in the angular extent was linked to the progression of retinal nerve fiber layer (RNFL) defects.[12,13] Ha et al. reported that the irregularity of the baseline β-zone PPA margin could be a marker for

0002-9394/$36.00
https://doi.org/10.1016/j.ajo.2024.05.032

vulnerability to glaucomatous damage.[14] Considering the limited research on baseline β-zone PPA morphology and its association with glaucoma progression, our study aims to provide crucial insights to enhance the understanding of PPA as a biomarker for glaucoma progression.

To elucidate the association between baseline β-zone PPA morphology and glaucoma progression, we utilized Optical Coherence Tomography (OCT) Guided Progression Analysis (GPA), a method employed in prior studies.[15-20] In the present study, inspired by the literature and using new morphological classification criteria, we investigated glaucoma progression based on OCT GPA according to baseline β-zone parapapillary atrophy (PPA) morphology in glaucoma patients.

METHODS

The study was approved by the Institutional Review Board (IRB) of SNUH complied with the tenets of the Declaration of Helsinki. The IRB (No. 2312-124-1494) waived the need for participants' informed consent owing to the study's retrospective nature.

• **STUDY PARTICIPANTS:** All of the participants visited SNUH's Glaucoma Clinic in Seoul, Korea, between January 2010 and December 2020. They were enrolled consecutively based on a retrospective medical-record review. We initially recruited 750 patients diagnosed with POAG. Subsequently, we classified a group of 524 patients in whom ß-zone PPA could be identified through fundus photography and OCT. Among them, patients with a follow-up period of less than 5 years and those who did not undergo sufficient glaucoma-related examinations suitable for this study were excluded. Ultimately, a final group of 210 patients was included in the analysis. The various criteria applied to select the final patient group will be described below.

On their initial visit to the Clinic, all of the participants underwent a full ophthalmic examination, including a medical history review, slit-lamp biomicroscopy, Goldmann applanation tonometry (Haag-Streit, Koniz Switzerland), gonioscopy, funduscopic examination (90 diopter lens), stereoscopic optic disk photography, red-free retinal nerve fiber layer (RNFL) photography, RNFL and optic nerve head (ONH) imaging by Cirrus spectral domain (SD)-OCT (Carl Zeiss Meditec, Dublin, CA, USA) and a central 24–2 threshold test of the Humphrey visual field (HVF) (HFA II; Humphrey Instruments Inc., Dublin, CA, USA).

The participants all had clearly detectable ß-zone PPA at baseline and had undergone RNFL and ONH imaging by Cirrus OCT every year for 5 or more years. Diagnosis of POAG was defined as follows: the presence of glaucomatous optic disk change (e.g., focal notching, thinning of rim, and RNFL defect), glaucomatous VF defect corresponding to structural change, and an open angle. ß-zone PPA was considered not to be a criterion for classification of glaucomatous optic neuropathy. The criteria for glaucomatous visual field (VF) defect were as follows: (1) a 3-point cluster of less than 5% probability in a typical location on a pattern deviation map, with at least one of the points having a less than 1% probability; (2) glaucomatous hemifield test results beyond the normal limits; or (3) pattern standard deviation greater than 95% of the normal limits, as confirmed on 2 or more examination results deemed to have been reliable (false-positives/false-negatives <15%, fixation losses <15%).

The POAG patients who met the following inclusion criteria were consecutively enrolled in the study: (1) more than 5 years of follow-up; (2) 5 or more consecutive RNFL photographs representative of the follow-up period; (3) baseline OCT scans with images clear enough for a visible scan circle and a signal strength of at least 6. The exclusion criteria were as follows: (1) history of intraocular surgery other than uncomplicated cataract surgery or history of disease(s) potentially impacting on the RNFL or VF examination results (e.g., ischemic optic neuropathy, diabetic retinopathy, uveitis, inflammatory disease, retinal vein occlusion, demyelinating disease, or pituitary lesion); (2) pallor of the optic disk; (3) media opacity (i.e., asteroid hyalosis, vitreous opacity, or significant cataract) rendering reading of diagnostic fundus imaging difficult; (4) advanced-stage glaucoma defined as the "severe" category of VF loss based on the Hodapp-Parrish-Anderson criteria. We required good-quality disk photographs and OCT images; poor-quality photographs that would render ß-zone PPA border identification difficult were excluded. In cases where both eyes proved eligible for inclusion, one was selected randomly.

• **MEASUREMENT OF PARAMETERS RELATED TO B-ZONE PARAPAPILLARY ATROPHY (PPA):** Presence of β-zone PPA was defined as a chorioretinal-atrophied area with visible sclera and optic-disk-adjacent choroidal vessels. Also, with the use of OCT, OCT defined β-zone PPA (with Bruch's membrane) and γ-zone PPA (without Bruch's membrane) were evaluated as previously described.[25] The parameters related to β-zone PPA were evaluated via stereoscopic optic disk photography, similarly to relevant previous studies.[11-13] The parameters were (1) maximal radial extent, (2) angular extent around the disk (circumference), and (3) β-zone PPA-to-disk-area ratio (PDR), as indicated in Figure 1. The pixel areas of β-zone PPA and clinical disk were obtained by ImageJ software (V.1.48; developed by Wayne Rasband, National Institute of Health, Bethesda, MD). The pixel areas (in square millimeters) were calculated by a formula for optic disk area correction using disk photography and spectral-domain OCT; this procedure has been described in detail by others.[21,22] All of the PPA parameters were measured independently by 2 glaucoma specialists. Images were evaluated in a masked fashion without knowledge of the patients' clinical diagnosis or any other clinical information.

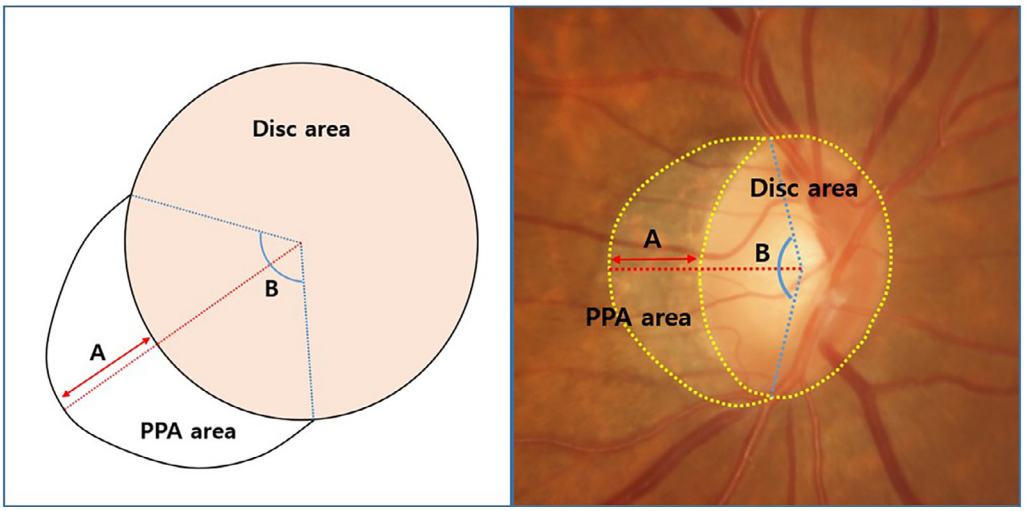

FIGURE 1. Measurement of ß-zone parapapillary atrophy (PPA) parameters. The parameters of ß-zone PPA were (A) maximal radial extent and (B) angular extent. The PPA area and disk area were each outlined manually (area within yellow dotted line), and the pixel area was calculated automatically using the software. The PPA-to-disk-area ratio (PDR) was obtained through the calculated pixel area ratio. (For interpretation of the references to color in this figure legend, the reader is referred to the web version of this article.)

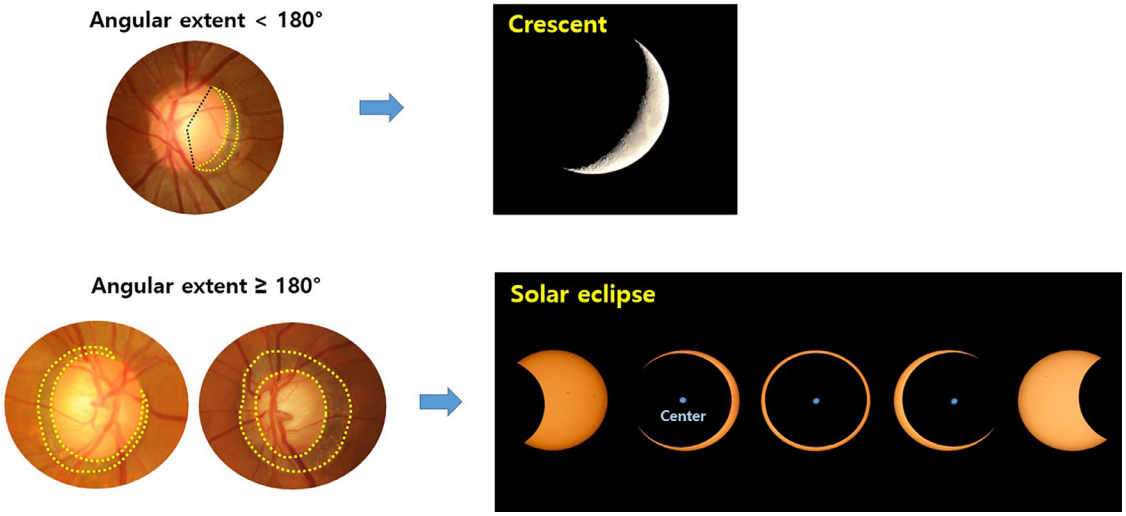

FIGURE 2-1. Idea of ß-zone PPA morphological classification based on angular extent. PPA with an angular extent of less than 180° resembles a crescent moon shape. When the angular extent was more than 180°, a similarity to the shape of a solar eclipse, where the moon blocks the sun, was noted. That is, if we assume that the center of the moon is a disk center, we can see that the shape of the PPA is similar to that of the light of the sun shining more than 180° around the moon.

The measurements were performed more than 3 times for each patient. The representative value was considered to be the average of those measurements.

• **CLASSIFICATION OF ß-ZONE PPA MORPHOLOGY:** In this study, we classified ß-zone PPA morphology according to a combination of PPA parameters, angular extent and radial extent. First, they were classified into “Crescent type” and “Solar-eclipse type” based on the 180-degree angular extent (Figure 2-1). Second, we classified the morphology of PPA once again based on the radial extent value, which is the average value of the population. If the radial extent was shorter than the average, PPA morphology was classified into "Type 1," and "Type 2" if longer (Figure 2-2, 2-3).

• **DEFINITION OF PROGRESSION ON GUIDED PROGRESSION ANALYSIS (GPA):** All of the OCT scans were acquired after pupillary dilatation using an internal fixation target.

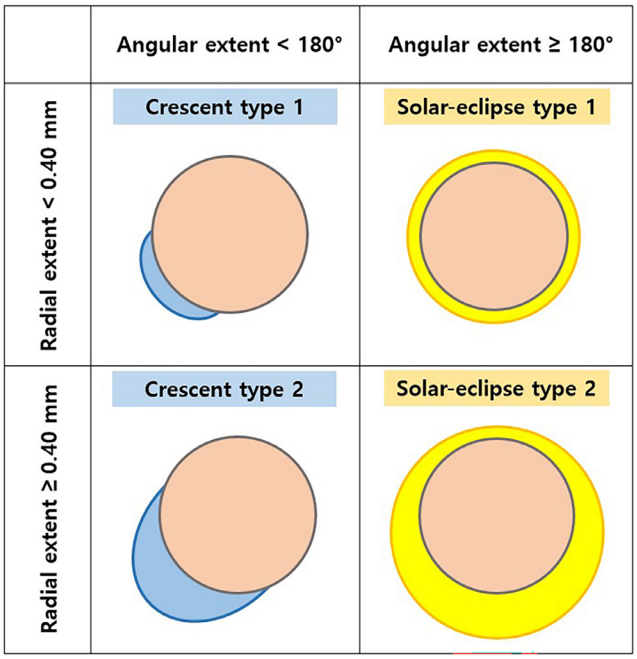

FIGURE 2-2. Model of ß-zone PPA type-classification criteria. First, ß-zone PPA was classified by angular extent. If it was less than 180°, it was named the Crescent type, and if it was more than 180°, it was named the Solar-eclipse type. Next, the ß-zone PPA type was classified once again, this time based on the average radial extent of the population, which is 0.4 mm. If the radial extent was shorter than 0.4 mm, it was named type 1, and if it was longer than 0.4 mm, it was named type 2.

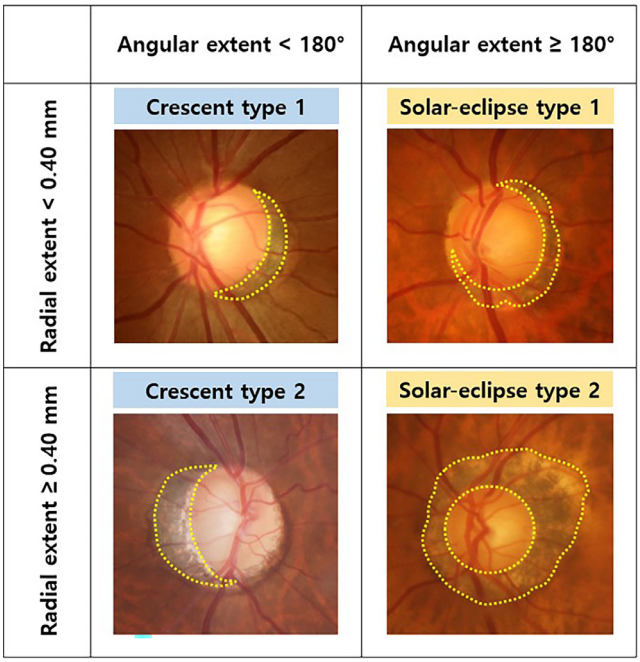

FIGURE 2-3. ß-zone PPA morphologies according to classification criteria. Various actual ß-zone PPA morphologies are classified according to the new classification criteria proposed in this study.

The Optic Disk Cube 200 × 200 scan protocol was applied. The Guided Progression Algorithm (OCT-GPA), which compares RNFL thickness between baseline and follow-up images, was used to generate a topographical display indicating the area and location of significant changes. The average thickness for the first two visits was taken as the baseline. If the change on follow-up exceeded the test–retest variability on visit or two visits, the pixel was coded in yellow (possible loss) or in red (likely loss), respectively. Based on these analyses, we defined GPA progression as the situation wherein "likely loss (coded in red)" was found in one or more of the following sectors: Average, Superior, and Inferior RNFL.

• **STATISTICAL ANALYSIS:** The data herein are presented as mean standard deviations (range) for normally distributed continuous variables; as median values with interquartile ranges for nonparametrically distributed continuous variables, and as frequencies (percentages) for categorical variables. Logistic regression models were used with the generalized estimating equation to investigate the factors related to progression on GPA. All of the variables showing associations with a P value of $< .05$ in the univariate regression analysis were included in the following binary multivariate regression analysis. In the analysis of the clinical characteristics of the four groups as classified by ß-zone PPA type, the P value were calculated with the use of one-way analysis of variance for normally distributed clinical characteristics, and by Fisher's exact test for categorical variables. All other data, which were nonparametrically distributed and recorded as median values with interquartile ranges, were analyzed with the use of the Kruskal-Wallis test for between-group comparisons, as well as the Mann-Whitney test for comparisons between pairs of groups when appropriate. All of the analyses were conducted using R Version 1.4.1717.

• **DECISION TREE ANALYSIS:** For a given dataset, decision tree models (DTMs) learn to predict the target variable according to decision rules inferred from the data features. Each decision rule is contained in each node. Every child node is connected to the question by the answer. The root node, the starting topmost node, is connected to the internal nodes. The internal nodes are divided into child nodes until leaf nodes are reached, and leaf nodes cannot be further divided by questions.

In the present study, a decision tree analysis was used to discriminate those patients with progression on GPA, using partitioning algorithms for age, sex, IOP, axial length, central corneal thickness, history of disk hemorrhage, and type of ß-zone PPA. We used the "ctree" function of the

TABLE 1. Comparison of Demographic and Baseline Clinical Characteristics Between Progressors and Non-Progressors

	Total ($N = 210$)	Non-Progressors ($N = 116$)	Progressors ($N = 94$)	*P*-Value
Demographic data				
Age (yrs)	53.8 ± 12.5	53.3 ± 12.1	54.4 ± 13.2	.54[b]
Male, *n* (%)	89 (42.4%)	52 (44.8%)	37 (39.4%)	.67[a]
Hypertension, *n* (%)	56 (26.7%)	31 (26.7%)	25 (26.6%)	1.00[a]
Diabetes mellitus, *n* (%)	28 (13.3%)	18 (15.5%)	10 (10.6%)	.46[a]
Follow-up duration (years)	9.8 ± 3.5	9.6 ± 3.7	10.2 ± 3.1	.12[b]
Clinical data				
Axial length (mm)	24.48 ± 1.42	24.54 ± 1.53	24.42 ± 1.29	.62[b]
Central corneal thickness (μm)	536.2 ± 38.0	537.3 ± 36.1	534.7 ± 40.6	.63[b]
Baseline IOP (mmHg)	14.8 ± 3.2	14.6 ± 3.2	15.1 ± 3.1	.27[b]
Mean deviation (dB)	−2.48 ± 2.89	−2.43 ± 2.90	−2.55 ± 2.89	.77[b]
OCT data				
Average RNFL thickness (μm)	80.2 ± 9.0	79.6 ± 8.6	80.9 ± 9.6	.33[b]
Inferior RNFL thickness (μm)	92.1 ± 18.6	90.3 ± 18.6	94.3 ± 18.3	.13[b]
Superior RNFL thickness (μm)	101.2 ± 17.6	99.8 ± 17.0	103.1 ± 18.2	.17[b]
Rim area (mm^2)	0.91 ± 0.17	0.91 ± 0.18	0.90 ± 0.17	.85[b]
Average CDR	0.71 ± 0.11	0.71 ± 0.11	0.71 ± 0.10	.59[b]
Vertical CDR	0.70 ± 0.11	0.70 ± 0.12	0.70 ± 0.11	.67[b]
Cup volume (mm^2)	0.44 ± 0.30	0.46 ± 0.32	0.42 ± 0.27	.44[b]

Data are the mean ± standard deviation (range) unless otherwise indicated.
IOP = intraocular pressure; RNFL = retinal nerve fiber layer; CDR = cup-to-disk ratio.
[a]The *P* values in the table refer to the comparison between the progressors and non-progressors.
[b]Student t-test or Mann-Whitney U test, *Chi-square test.

"party" R software package (version 4.0.5; default settings). A decision tree was split by these variables in a hierarchical manner until leaf nodes were reached.

RESULTS

• **DEMOGRAPHICS, BASELINE CLINICAL CHARACTERISTICS, AND FOLLOW-UP CHARACTERISTICS:** A total of 210 eyes of 210 patients with an average follow-up of 9.8 ± 3.5 years were included in the present study. Their average age at the initial visit was 53.8 ± 12.5 years. No differences were observed regarding age, sex, baseline intraocular pressure (IOP), axial length (AXL), central corneal thickness (CCT) or mean deviation (MD) between progressor and non-progressor groups. Even in the OCT data, there were no intergroup differences in baseline RNFL thickness, rim area, cup-to-disk ratio (CDR) or cup volume (Table 1). However, radial extent, angular extent and PPA-to-disk area ratio (PDR) showed, in a comparative analysis of the parameters related to β-zone PPA, significant differences (Table 2). There was no intergroup difference in mean IOP during the follow-up period. Likewise, there was no difference in maximum, minimum IOP or IOP fluctuation. However, disk hemorrhage was more frequent in the progressor group (Table 3).

• **PROGRESSION ON OCT GPA AND RELATED FACTORS:** As for the logistic regression analysis models, in the univariate analysis, disk hemorrhage, radial extent, angular extent and PDR were all found to be significantly associated with progression on GPA ($P = .035$, $P < .001$, $P < .001$, and $P = .002$). In the multivariate analysis, both radial extent and angular extent were found to be significantly associated with progression on GPA ($P < .001$, $P < .001$) (Table 4).

• **PROGRESSION ON OCT GPA ACCORDING TO PPA TYPE:** There were no differences observed in age, gender, AXL, or disk hemorrhage among the four types of PPA. Nevertheless, discrepancies were noted in OCT GPA progression. Post hoc analysis revealed significant differences between Crescent type 1 and the other three types, as well as between Solar-eclipse type 1 and Solar-eclipse type 2. The rate of RNFL change also exhibited differences, with variations in the change rates of average, superior, and inferior RNFL thickness between Crescent type 1 and Solar-eclipse type 2 (Table 5). A Kaplan-Meier survival curve showed differences in the rates of progression on GPA between the 4 types of PPA. The median survival line showed rapid progression in the following order: Solar-eclipse type 2, Crescent type 2, Solar-eclipse type 1, Crescent type 1 (Figure 3).

TABLE 2. Comparison of ß-Zone Parapapillary Atrophy Parameters Between Progressors and Non-Progressors

	Total ($N = 210$)	Non-Progressors ($N = 116$)	Progressors ($N = 94$)	*P*-Value
ß-zone PPA parameter				
Radial extent (mm)	0.39 ± 0.20	0.33 ± 0.15	0.47 ± 0.23	**< .001**
Angular extent (°)	210.9 ± 79.1	190.5 ± 75.1	237.0 ± 76.7	**< .001**
PPA-to-disk-area ratio	0.46 ± 0.37	0.38 ± 0.30	0.57 ± 0.43	**< .001**

Data are recorded as mean ± standard deviation.
PPA = parapapillary atrophy.
The *P* values were calculated by Student t-test or Mann-Whitney U test.

TABLE 3. Comparison of Follow-Up Characteristics Between Progressors and Non-Progressors

	Total ($N = 210$)	Non-Progressors ($N = 116$)	Progressors ($N = 94$)	*P*-Value
Mean IOP (mmHg)	12.7 ± 1.7	12.6 ± 1.6	12.8 ± 1.7	.86[a]
Maximum IOP (mmHg)	15.2 ± 2.4	15.0 ± 2.3	15.3 ± 2.1	.85[a]
Minimum IOP (mmHg)	9.2 ± 2.1	9.2 ± 2.0	9.3 ± 2.4	.91[a]
IOP fluctuation (mmHg)	1.5 ± 0.9	1.5 ± 0.9	1.5 ± 0.8	.87[a]
Optic disk hemorrhage, *n* (%)	71 (33.8%)	32 (27.6%)	39 (41.5%)	**.002**[b]

Bold value indicates P < 0.05.
Data are the mean ± standard deviation (range) unless otherwise indicated.
IOP = intraocular pressure.
[a]Student t-test or Mann-Whitney U test.
[b]Chi-square test.

TABLE 4. Univariate and Multivariate Logistic Regression Analysis for Progression on OCT GPA

	Univariate		Multivariate	
	Odds Ratio (95% CI)	*P*-Value	Odds Ratio (95% CI)	*P*-Value
Demographic variables				
Age	1.01 (0.98-1.03)	.57		
Sex	1.25 (0.72-2.18)	.43		
Hypertension	0.99 (0.53-1.84)	.98		
Diabetes mellitus	0.65 (0.27-1.46)	.30		
Follow-up duration (years)	1.05 (0.97-1.14)	.21		
Clinical variables				
Axial length	0.94 (0.74-1.17)	.57		
Central corneal thickness	1.00 (0.99-1.00)	.47		
Baseline IOP	1.04 (0.96-1.14)	.33		
Mean IOP	1.05 (0.97-1.15)	.42		
IOP fluctuation	1.04 (0.97-1.14)	.38		
Disc hemorrhage	1.86 (1.05-3.33)	**.035**	1.84 (0.98-3.47)	.06
PPA parameters				
Radial extent	1.53 (1.28-1.87)	**< .001**	1.70 (1.33-2.23)	**< .001**
Angular extent (°)	1.01 (1.00-1.01)	**< .001**	1.01 (1.00-1.01)	**< .001**
PPA-to-disk-area ratio	4.25 (1.79-11.35)	**.002**	0.34 (0.09-1.35)	.10

Bold value indicates P < 0.05.
OCT = optic coherence tomography; GPA = guided progression analysis; CI = confidence interval; IOP = intraocular pressure; PPA = parapapillary atrophy.

TABLE 5. Comparison of Characteristics Between 4 PPA Types

	Crescent Type 1 ($N = 60$)	Crescent Type 2 ($N = 43$)	Solar-Eclipse Type 1 ($N = 49$)	Solar-Eclipse Type 2 ($N = 58$)	*P*-Value
Age	54.3 ± 13.6	53.6 ± 11.5	58.7 ± 9.9	55.1 ± 11.2	.38
Axial length (mm)	24.05 ± 1.29	25.13 ± 1.18	23.70 ± 0.92	24.96 ± 1.62	.12
CCT (μm)	541.3 ± 32.2	539.6 ± 34.9	524.4 ± 38.6	537.3 ± 44.2	.14
Baseline MD (dB)	-2.09 ± 3.11	-2.66 ± 2.73	-2.23 ± 2.66	-2.96 ± 2.94	.21
Disk hemorrhage, *n* (%)	13 (21.7%)	15 (34.9%)	17 (34.7%)	22 (37.9%)	.14
OCT data					
Baseline RNFL thickness					
Average thickness (μm)	79.4 ± 9.5	80.6 ± 8.7	80.5 ± 9.6	80.3 ± 8.4	.88
Superior thickness (μm)	101.6 ± 18.1	100.2 ± 16.1	103.3 ± 19.1	99.9 ± 17.1	.88
Inferior thickness (μm)	92.4 ± 19.6	91.0 ± 15.4	95.8 ± 18.6	89.3 ± 19.4	.20
Change rate of RNFL					
Average RNFL (μm/yr)	-0.99 ± 0.78	-1.31 ± 1.21	-1.15 ± 1.42	-1.43 ± 0.69	**.001**[1-4, 3-4]
Superior RNFL (μm/yr)	-1.52 ± 1.45	-1.79 ± 1.78	-1.54 ± 2.14	-1.89 ± 1.32	**.046**[1-4]
Inferior RNFL (μm/yr)	-1.30 ± 1.11	-2.05 ± 1.68	-2.02 ± 2.52	-2.16 ± 1.32	**.001**[1-4]
GPA progression, *n* (%)	10 (16.6%)	21 (48.8%)	21 (42.9%)	42 (72.4%)	**< .001**[1-2, 1-3, 1-4, 3-4]

Bold value indicates $P < 0.05$.

Data are the mean ± standard deviation (range) unless otherwise indicated.

PPA = parapapillary atrophy; CCT = central corneal thickness; MD = mean deviation; OCT = optic coherence tomography; RNFL = retinal nerve fiber layer; GPA = guided progression analysis.

Next to the *P*-value of less than .05, the group in which there was a difference through post hoc analysis is indicated. (1 = Crescent type 1, 2 = Crescent type 2, 3 = Solar-eclipse Type 1, 4 = Solar-eclipse Type 2).

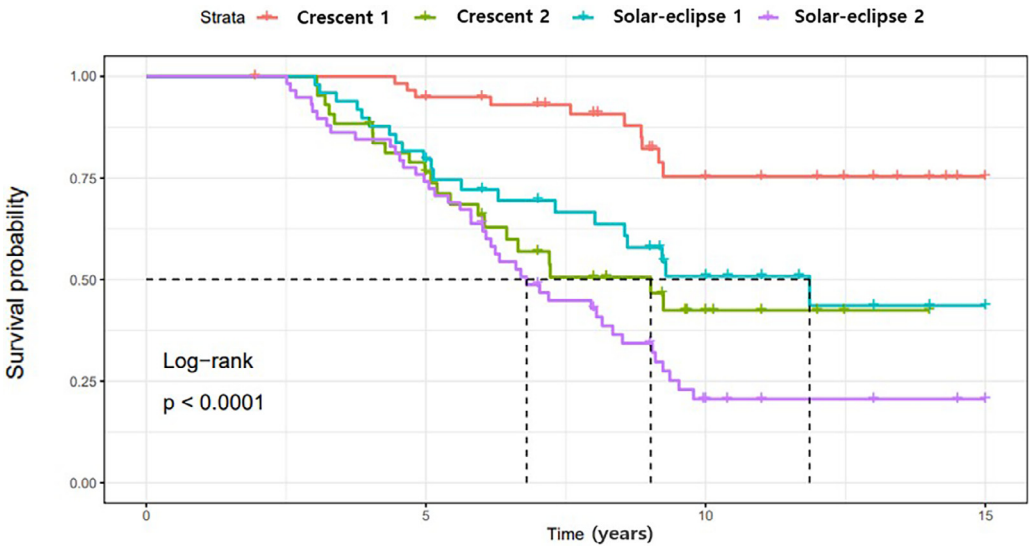

FIGURE 3. Kaplan-Meier survival curve. The Kaplan-Meier survival curve shows the survival rate of progression on guided progression analysis (GPA) according to the 4 ß-zone PPA morphology types. Differences in survival rates were seen depending on the 4 types, and differences in median survival time (black dotted line) also were seen.

• **DECISION TREE ANALYSES:** The decision tree model (DTM) results for prediction of progression on GPA are plotted in Figure 4. Among the candidate variables (age, sex, IOP, AXL, CCT, baseline MD, disk hemorrhage, and PPA type), only disk hemorrhage and PPA type were identified as decision nodes determinative of progression on GPA. According to the DTM, (1) Crescent type 1 was predicted to have less progression than the remaining three types, and (2) Solar-eclipse type 2 was strongly predicted to progress more than the remaining three types. (3) Crescent type 2 and Solar-eclipse type 1 were predicted to progress more when disk hemorrhage is present in both groups, and between the two groups, (4) Crescent type 2 was predicted to show further progression.

DISCUSSION

The results of this longitudinal observational study shed light on the relationship between ß-zone PPA morphology and glaucoma progression, as assessed on OCT GPA in POAG patients. Understanding this relationship is essential for early glaucoma detection and management.

The parapapillary atrophy surrounds the optic nerve head and has been differentiated into alpha zone and beta zone,[23] More recently, it was differentiated into gamma zone and delta zone.[24] The classic β-zone PPA was subdivided into newly defined β-zone PPA with Bruch's membrane and γ-zone PPA without overlying Bruch's membrane.[24] Among these, the β-zone PPA has been found to be related to glaucoma in several studies, and the γ-zone PPA was related to myopic change rather than glaucomatous change.[25,26] The association of β-zone PPA and glaucoma has been widely studied using morphometric techniques. In fact the presence of β-zone PPA, which increases the risk of glaucoma progression,[27,28] is useful for the purposes of early diagnosis of glaucoma.[29-31] Therefore, in this study, we analyzed the β-zone PPA area of glaucoma patients, newly classified the shape of β-zone area, and analyzed the clinical course.

This study found that several parameters related to β-zone PPA, including radial extent, angular extent, and PPA-to-disk-area ratio (PDR), showed significant differences between progressor and non-progressor groups. These findings suggest a strong correlation between ß-zone PPA morphology at baseline and the glaucoma progression. PPA has long been associated with glaucoma development and progression, and indeed, this study reinforces its importance as a predictive factor. Logistic regression analysis identified disk hemorrhage, radial extent, and angular extent as significant factors associated with progression on GPA. disk hemorrhage is a well-established risk factor for glaucoma progression, and its presence in the findings of this study further supports this relationship. The radial and angular extents of PPA provide quantitative measures of PPA morphology, and their significance in predicting glaucoma progression highlights the importance of assessing PPA characteristics in glaucoma patients.

Teng et al. reported that the location of largest β-zone PPA typically correlates spatially with the region of the most rapid future VF progression.[11] However, this study did not analyze the location of the largest beta zone and its correlation with glaucoma progression. This aspect was excluded from the analysis because the primary aim of this study was to determine the effect of morphological characteristics of PPA on glaucoma progression. Nevertheless, as the aforementioned study results suggest, the location of the PPA may potentially influence glaucoma progression. Therefore, future analyses will be necessary to combine the morphological classification presented in this study with the location of the PPA.

This study classified ß-zone PPA morphology into "Crescent type" and "Solar-eclipse type" based on angular extent and "type 1″ and "type 2″ based on radial extent. This classification approach provides a valuable framework for understanding and categorizing ß-zone PPA characteristics. The significant differences in glaucoma progression and RNFL change rate among these ß-zone PPA types further emphasize the clinical relevance of PPA morphology. Our results suggest that the frequency and rate of glaucoma progression will be higher and faster in ß-zone PPA types with larger radial and angular extents. Furthermore, in the comparison between Crescent type 2 (PPA with only longer radial extent) and Solar-eclipse type 1 (PPA with only larger angular extent), it is anticipated that Crescent type 2 will lead to a faster and more frequent progression of glaucoma. Although the exact mechanisms underlying these findings remain unclear, ß-zone PPA area likely reflects the vascular and mechanical vulnerability of the area surrounding the ONH. Indeed, the prelaminar portion of the ONH receives its blood supply primarily from the peripapillary choroid through branches of the short posterior ciliary artery, which have a characteristic sectoral distribution.[32-34]

The criteria we presented for ß-zone PPA classification may appear to correlate with the size of PPA. For instance, when comparing Crescent type 1 (with shorter radial extent and smaller angular extent) to Solar-eclipse type 2 (with longer radial extent and larger angular extent), there seems to be a clear difference in size. However, when comparing Crescent type 2 (with longer radial extent) to Solar-eclipse type 1 (with larger angular extent), it becomes evident that the shape of the PPA protrudes significantly from the disk margin or encompasses the disk margin widely, rather than strictly correlating with size. Therefore, the criteria we presented primarily reflect the form or shape of the PPA, rather than its size.

The decision tree analysis provided valuable insights into predictive factors for glaucoma progression, highlighting disk hemorrhage and PPA type as key determinants affecting progression in GPA. This analysis offers a practical tool for assessing the risk of glaucoma progression based on easily identifiable factors.

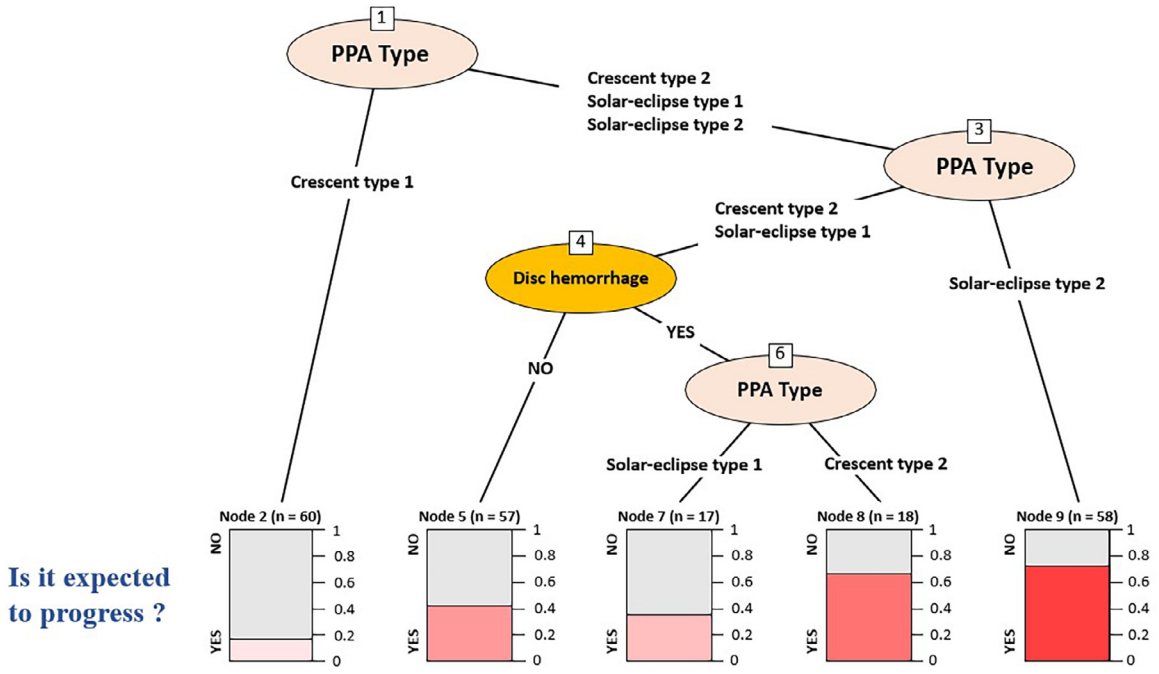

FIGURE 4. Decision tree model (DTM) of progression on guided progression analysis (GPA). Using the ß-zone PPA classification criteria newly proposed in this study, we analyzed and created a decision tree model for prediction of glaucoma progression frequency. First, Crescent type 1 was predicted to progress less than the other three types, and among the remaining three types, Solar-eclipse type 2 had the highest predicted frequency. Second, Crescent type 2 and Solar-eclipse type 1 showed differences in predicted frequency depending on the presence of disk hemorrhage. (For interpretation of the references to color in this figure legend, the reader is referred to the web version of this article.)

The present study has several limitations that should be acknowledged. First, the subjects were recruited from one tertiary referral hospital and were exclusively of Korean ethnicity, which may have introduced potential selection biases and restricted the generalizability of the findings. Replication of the study in diverse populations would enhance the external validity of the results. Second, measurements were performed with disk photographs, which are flattened projections of the curved surface of the eye, therefore, errors could have been incurred. Also, ß-zone PPA and parameters related to PPA were determined in a subjective manner, which could have resulted in a slight degree of measurement variability. However, because we required repeated measurements between 2 masked reviewers, the inter-reader agreement for all of the PPA parameters was excellent. We differentiated the beta zone from the alpha zone and gamma zone using fundus photography and OCT. Jonas et al.[35] histologically differentiated between myopic beta zone and glaucomatous beta zone. However, in this study, only fundus photography and OCT were utilized, thus there are limitations in distinguishing between myopic and glaucomatous beta zones. Nevertheless, future studies should consider analyzing the clinical course of glaucoma based on distinctions between myopic and glaucomatous beta zones. Third, we analyzed glaucoma progression only by changes in RNFL thickness. There are structural and functional test methods using various equipment to evaluate glaucoma progression, but it is difficult to achieve uniformity in the evaluation of progression if multiple test methods are included. For this reason, RNFL thickness change was chosen as the representative method, as the RNFL is not only in close proximity to the ONH but also provides a comprehensive measure of structural changes associated with glaucoma progression. Fourth, the follow-up period varied among patients, potentially leading to a missed identification of later-occurring progression in those with a shorter follow-up. However, this study aimed to address these limitations by comparing the rate of change using both OCT GPA and survival analysis.

In conclusion, this longitudinal observational study highlights the crucial role of ß-zone PPA morphology in predicting glaucoma progression in POAG patients. The findings emphasize the significance of assessing ß-zone PPA characteristics, including radial extent, angular extent, and PDR, as potential indicators of glaucoma progression.

Classification of ß-zone PPA into "Crescent type" and "Solar-eclipse type," along with "type 1″ and "type 2″ based on radial extent, provides a useful framework for characterizing PPA morphology. These classifications enable

clinicians to stratify glaucoma patients into risk groups, thereby facilitating more targeted and personalized treatment strategies. Decision tree analysis as demonstrated herein further simplifies risk assessment by identifying disk hemorrhage and PPA type as the primary determinants of progression on GPA. This approach, allowing for early intervention in the cases of patients at higher risk of glaucoma progression, has crucial practical implications for clinical practice. Further research and validation studies may refine the use of PPA morphology as a predictive tool in clinical practice, ultimately improving early detection and management of glaucoma.

CREDIT AUTHORSHIP CONTRIBUTION STATEMENT

MIN GU HUH: Writing – original draft, Methodology, Investigation, Formal analysis, Data curation, Conceptualization. **YOON JEONG:** Formal analysis, Data curation, Conceptualization. **YOUNG IN SHIN:** Writing – review & editing, Supervision, Data curation. **KI HO PARK:** Writing – review & editing, Supervision. **JIN WOOK JEOUNG:** Writing – review & editing, Supervision, Resources, Methodology, Conceptualization.

Funding/Support: This research did not receive any specific grant from funding agencies in the public, commercial, or not-for-profit sectors.
Financial Disclosures: no conflicting relationship exists for any author.

REFERENCES

1. Jonas JB, Nguyen XN, Gusek GC, Naumann GO. Parapapillary chorioretinal atrophy in normal and glaucoma eyes. I. Morphometric data. *Invest Ophthalmol Vis Sci*. 1989;30:908–918.
2. Jonas JB. Clinical implications of peripapillary atrophy in glaucoma. *Curr Opin Ophthalmol*. 2005;16:84–88.
3. Anderson DR, Braverman S. Reevaluation of the optic disk vasculature. *Am J Ophthalmol*. 1976;82:165e–1174.
4. Anderson DR. Correlation of the peripapillary anatomy with the disc damage and field abnormalities in glaucoma. *Doc Ophthalmol Proc Ser*. 1983;35:1–10.
5. Rockwood EJ, Anderson DR. Acquired peripapillary changes and progression in glaucoma. *Graefes Arch Clin Exp Ophthalmol*. 1988;226:510–515.
6. Uchida H, Ugurlu S, Caprioli J. Increasing peripapillary atrophy is associated with progressive glaucoma. *Ophthalmology*. 1998;105:1541–1545.
7. Budde WM, Jonas JB. Enlargement of parapapillary atrophy in follow-up of chronic open-angle glaucoma. *Am J Ophthalmol*. 2004;137:646–654.
8. Kwon YH, Kim YI, Pereira ML, et al. Rate of optic disc cup progression in treated primary open-angle glaucoma. *J Glaucoma*. 2003;12:409–416.
9. Tezel G, Kass MA, Kolker AE, et al. Comparative optic disc analysis in normal pressure glaucoma, primary open-angle glaucoma, and ocular hypertension. *Ophthalmology*. 1996;103:2105–2113.
10. Park KH, Tomita G, Liou SY, Kitazawa Y. Correlation between peripapillary atrophy and optic nerve damage in normal-tension glaucoma. *Ophthalmology*. 1996;103:1899–1906 .
11. Teng CC, De Moraes CG, Prata TS, et al. The region of largest beta-zone parapapillary atrophy area predicts the location of most rapid visual field progression. *Ophthalmology*. 2011;118:2409–2413.
12. Bak E, Ha A, Kim YW, et al. Ten years and beyond longitudinal change of ß-zone parapapillary atrophy: comparison of primary open-angle glaucoma with normal eyes. *Ophthalmology*. 2020;127:1054–1063.
13. Bak E, Kim YW, Kim YK, Park KH. Ten-year-and-beyond longitudinal change of ß-zone parapapillary atrophy in glaucoma: association with retinal nerve fiber layer defect. *Br J Ophthalmol*. 2022;106:1393–1398.
14. Ha A, Kim YW, Lee J, et al. Morphological characteristics of parapapillary atrophy and subsequent visual field progression in primary open-angle glaucoma. *Br J Ophthalmol*. 2021;105:361–366.
15. Na JH, Sung KR, Baek S, et al. Progression of retinal nerve fiber layer thinning in glaucoma assessed by cirrus optical coherence tomography-guided progression analysis. *Curr Eye Res*. 2013;38:386–395.
16. Shin JW, Sung KR, Lee GC, et al. Ganglion cell-inner plexiform layer change detected by optical coherence tomography indicates progression in advanced glaucoma. *Ophthalmology*. 2017;124:1466.1474.
17. Miki A, Medeiros FA, Weinreb RN, et al. Rates of retinal nerve fiber layer thinning in glaucoma suspect eyes. *Ophthalmology*. 2014;121:1350–1358.
18. Tenkumo K, Hirooka K, Baba T, et al. Evaluation of relationship between retinal nerve fiber layer thickness progression and visual field progression in patients with glaucoma. *Jpn J Ophthalmol*. 2013;57:451–456.
19. Leung CK, Yu M, Weinreb RN, et al. Retinal nerve fiber layer imaging with spectral-domain optical coherence tomography: patterns of retinal nerve fiber layer progression. *Ophthalmology*. 2012;119:1858–1866.
20. Shin JW, Sung KR, Lee J, et al. Factors associated with visual field progression in cirrus optical coherence tomography-guided progression analysis: a topographic approach. *J Glaucoma*. 2017;26:555–560.
21. Kim YK, Park KH, Yoo BW, Kim HC. Topographic characteristics of optic disc hemorrhage in primary open-angle glaucoma. *Invest Ophthalmol Vis Sci*. 2014;55:169–176.
22. Park HY, Lee K, Park CK. Optic disc torsion direction predicts the location of glaucomatous damage in normal-tension glaucoma patients with myopia. *Ophthalmology*. 2012;119:1844–1851.
23. Jonas JB, Fernandez MC, Naumann GO. Glaucomatous parapapillary atrophy: occurrence and correlations. *Arch Ophthalmol*. 1992;110:214–222.

24. Jonas JB, Jonas SB, Jonas RA, et al. Parapapillary atrophy: histological gamma zone and delta zone. *PLoS One*. 2012;7:e47237.
25. Dai Y, Jonas JB, Huang H, et al. Microstructure of parapapillary atrophy: beta zone and gamma zone. *Invest Ophthalmol Vis Sci*. 2013;54:2013–2018.
26. Kim M, Kim T-W, Weinreb RN, et al. Differentiation of parapapillary atrophy using spectral-domain optical coherence tomography. *Ophthalmology*. 2013;120:1790–1797.
27. Lee EJ, Kim TW, Weinreb RN, et al. β-Zone parapapillary atrophy and the rate of retinal nerve fiber layer thinning in glaucoma. *Invest Ophthalmol Vis Sci*. 2011;52:4422–4427.
28. Teng CC, De Moraes CGV, Prata TS, et al. β-zone parapapillary atrophy and the velocity of glaucoma progression. *Ophthalmology*. 2010;117:909–915.
29. Tezel G, Kolker AE, Kass MA, et al. Parapapillary chorioretinal atrophy in patients with ocular hypertension. I. An evaluation as a predictive factor for the development of glaucomatous damage. *JAMA Ophthalmol*. 1997;115:1503–1508.
30. Tezel G, Kolker AE, Wax MB, et al. Parapapillary chorioretinal atrophy in patients with ocular hypertension. II. An evaluation of progressive changes. *JAMA Ophthalmol*. 1997;115:1509–1514.
31. Jonas JB, Budde WM. Diagnosis and pathogenesis of glaucomatous optic neuropathy: morphological aspects. *Prog Retin Eye Res*. 2000;19:1–40.
32. Lieberman MF, Maumenee AE, Green WR. Histologic studies of the vasculature of the anterior optic nerve. *Am J Ophthalmol*. 1976;82:405–423.
33. Hayreh SS. Blood supply of the optic nerve head and its role in optic atrophy, glaucoma, and oedema of the optic disc. *Br J Ophthalmol*. 1969;53:721–748.
34. Hayreh S. The optic nerve head circulation in health and disease. *Exp Eye Res*. 1995;61:259–272.
35. Jonas JB, Jonas RA, Jonas SB, et al. Myopic versus glaucomatous parapapillary beta zone in myopic eyes versus eyes with secondary angle-closure glaucoma. *Invest Ophthalmol Vis Sci*. 2023;64:25.